Journal of Non-Crystalline Solids 431 (2016) 36–40

Contents lists available at ScienceDirect

Journal of Non-Crystalline Solids

journal homepage: www.elsevier.com/ locate/ jnoncrysol

Laser-induced growth of oriented Sb_2S_3 single crystal dots on the surface of 82SbSI–18Sb_2S_3 glasses

D. Savytskii [a], B. Knorr [b], V. Dierolf [b], H. Jain [a,*]

[a] Department of Materials Science and Engineering, Lehigh University, 5 East Packer Avenue, Bethlehem, PA 18015, USA
[b] Department of Physics, Lehigh University, 16 Memorial Drive East, Bethlehem, PA 18015, USA

ARTICLE INFO

Article history:
Received 29 November 2014
Accepted 2 March 2015
Available online 16 March 2015

JEL classifications:
61.05.Jm
61.80.Ba
68.35.Bj
81.10.Jt

Keywords:
Chalcogenide glass;
CW laser;
Crystallization

ABSTRACT

To produce ferroelectric single-crystal architecture on glass surface by laser irradiation, usually the starting structure is a dot. Therefore, we have investigated the formation of this basic element of laser-induced crystallization, as an example, on the surface of pseudo binary 82SbSI–18Sb_2S_3 chalcogenide glass using a diode laser of wavelength $\lambda = 520$ nm. The intensity of the laser was chosen such that the temperature in the crystal growth region was kept below the melting temperature of the glass but high enough to facilitate solid state devitrification. The morphology, crystallinity and composition of crystallized dots were determined using Electron Backscatter Diffraction (EBSD) and Energy Dispersive X-ray Spectroscopy (EDS). We find that Sb_2S_3 single crystal dots with elliptic cross-section form with <001> direction parallel to the major axis of ellipse and the surface of glass matrix. On the basis of the presented results, we propose that laser heating can be exploited uniquely to grow oriented single crystals of solids.

1. Introduction

Crystallization of glass by CW laser irradiation is a novel method which is recognized for its potential to construct active elements and devices. Thus far this technique has been applied primarily to oxide glass insulators [1,2]. By contrast, chalcogenide glasses are 'soft', wide bandgap semiconductors, which show strong electron–phonon coupling and photosensitivity. Consequently, laser-induced crystallization of chalcogenide is expected to be significantly more complex [3]. Basic structural elements like zero-dimensional dots, one-dimensional (1D) lines and two-dimensional (2D) rectangles of single crystals have been written at or near the surface by selectively heating the glass with a laser beam that is absorbed by the glass matrix [1–3]. At present, a complete mechanistic understanding of this laser-induced crystal growth process is lacking. Obviously, one would benefit by answering the question: how does the simplest structure, viz. a dot, form in or on glass upon exposure to suitable laser.

Antimony trisulfide (Sb_2S_3) is a promising material for photovoltaic cells since it shows high absorption coefficient ($\alpha > 10^3$ cm^{-1}), and the bandgap (1.7–2.5 eV) covers the maximum scan of the visible and near infrared ranges of the solar spectrum [4]. On the other hand, Sb_2S_3 has attracted attention for its applications in thermoelectric and optoelectronic devices operating in the infrared (IR) region [5,6]. It is a highly anisotropic material with a layer structure and strong tendency to form 1-D structures. There is a great interest in preparing Sb_2S_3 nanostructures as nanorods, nanowires, and nanoribbons, among other morphologies, using a wide variety of procedures [7–9]. Therefore, we have selected to understand laser-induced formation of dots in this glass.

For forming single crystal of Sb_2S_3 in glass, it is important to choose a composition that satisfies two conditions: forms into glass easily and crystallizes in Sb_2S_3 phase when taken to peak crystallization temperature. These requirements of chemical composition are well satisfied by 82SbSI–18Sb_2S_3. It corresponds to the edge of glass forming region within the Sb–S–I system. In this paper, we report results in the laser patterning of crystalline dots on the surface of the glasses of 82SbSI–18Sb_2S_3 under irradiation with a 520 nm CW laser diode in air. The wavelength 520 nm is above the bandgap of the selected glass composition, and is thus absorbed within a thin surface layer (several hundred nanometers) of the sample. Consequently, we can expect that the maximum temperature from laser heating will be located near the surface of sample.

2. Experimental

2.1. Sample preparation

We prepared glasses starting with a batch of elemental Sb, S and I powders in appropriate ratio, and following the ampule quenching method previously developed for the SbSI–GeS_2 system [10]. 82SbSI–

* Corresponding author.
E-mail address: hj00@Lehigh.EDU (H. Jain).

http://dx.doi.org/10.1016/j.jnoncrysol.2015.03.007
0022-3093/

$18Sb_2S_3$ glass, which is within the normal glass-forming region of the Sb–S–I system, was prepared. The glass of non-stoichiometric composition was prepared using ampules with 11 mm ID. X-ray powder diffraction (XRD) analysis of the as-quenched samples confirmed their amorphous state.

The sample surfaces for laser treatments were prepared using metallographic polishing techniques. First, plate-like samples were ground using 600-, 1000- and 1200-grit SiC abrasive papers in conjunction with water as lubricant. Next, the flat samples were polished using Al_2O_3 suspensions with particle sizes of 3, 1, 0.3, 0.1 and 0.05 μm.

2.2. Laser writing setup

We started with the fabrication of crystal dots using a λ = 520 nm ThorLabs LP520-SF15 single mode fiber pigtailed laser diode. This laser provided the ability to precisely control the intensity using ILK Lightwave LDX-3620 Ultra Low Noise Current Source with an analog control input. Using a microscope objective (numerical aperture 0.75) illuminated spots of 5 μm diameter were produced on the polished surface of the glass sample. Crystallized dots were created by slowly ramping the power density from 0 to 80 μW/μm^2 within a time period. Upon reaching final power (80 μW/μm^2), the laser was held in place at the same spot for an additional length of time.

2.3. Characterization of laser written structures

The laser-irradiated regions were analyzed with a Scanning Electron Microscope (Hitachi 4300 SE) in water vapor environment to minimize the charging effects. Chemical composition of samples was determined by an Energy Dispersive X-ray (EDS) spectroscopy detector attached to SEM. The parameters for data acquisition (acceleration voltage, time, full scale for intensity, pulse processing time) were kept the same for all the samples. The spectra were collected for separate points on a sample's surface and analyzed using EDAX-Genesis software package. A qualitative color map of the distribution of major elements as well as oxygen in the laser-irradiated regions was obtained using the same EDAX software.

Crystallinity and orientation of the crystal grains in laser created dots were examined by Electron Backscatter Diffraction (EBSD) technique, in which Kikuchi patterns were collected by a Hikari detector inserted into the SEM specimen chamber. The crystalline grains and their orientation within selected areas were determined through EBSD mapping scans. The step size for these maps was 0.2 μm with a hexagonal sampling grid. EBSD scans were collected and indexed using TSL (TexSEM Laboratory) orientation data collection and analysis software. All patterns were indexed using SbSI and Sb_2S_3 crystal structure parameters. Indexing of diffraction patterns was achieved by a voting system and characterized by a number of parameters such as the image quality (IQ) value votes, the fit-factor, and the confidence index (CI). The orientation imaging microscopy (OIM) software package was used to identify crystal grains and generate image quality, phase, and inverse as well as normal pole figure maps. All these maps were filtered for CI < 0.1.

3. Results

3.1. Thermally induced crystallization of glasses in the Sb–S–I system

In order to understand laser-induced crystallization, it is instructive to know how a given glass composition would transform upon simple heating. Therefore, ordinary temperature induced crystallization of Sb–S–I glasses within the $xSbSI–(100–x)Sb_2S_3$ pseudo-binary series was investigated in our group previously [11,12]. The differential scanning calorimetric scans and X-ray diffraction measurements on the powders of these compositions of varying size particles allowed the identification of one-dimensional (1D) surface, and three-dimensional (3D) bulk crystallizations of the SbSI phase, which depended on the composition of the glass [11]. Similar to the case of stoichiometric SbSI (G1) glass, SbSI phase devitrifies by the two crystallization processes in other glasses within $xSbSI–(100–x)Sb_2S_3$ [12]. This result is shown in Fig. 1. With decreasing SbSI concentration, *x*, we find that the two exothermal effects shift to higher temperatures and the temperature interval between them decreases. In contrast to the SbSI phase, the temperature of crystallization for the Sb_2S_3 phase does not depend on the size of particles and slowly decreases with decreasing *x*. For $63SbSI–37Sb_2S_3$ (G3) glass, which corresponds to eutectic composition, the temperature of SbSI bulk crystallization becomes higher than the crystallization point of Sb_2S_3 phase. Evidently, for the glass of $52SbSI–48Sb_2S_3$ (G4) composition Sb_2S_3 phase starts to crystallize first. This completely changes the conditions for nucleation and further crystallization of both the phases in glasses with the hypereutectic chemical composition.

3.2. Laser-induced single crystal dots in $82SbSI–18Sb_2S_3$ glass (G2)

We investigated structural and chemical changes induced by the 520 nm CW laser beam in a dot for different exposure conditions: ramping the power density from zero to 80 μW/μm^2 in 5 or 10 s with or without additional exposure for 5 s or 10 s. For comparison, we also produced a dot irradiated with 50 μW/μm^2 intensity at once for 5 s.

Fig. 2 shows typical morphology of dots produced on $82SbSI–18Sb_2S_3$ glass, where we see two different depressed or contracted regions: inner area (*B*) irradiated by the laser beam, and an area *A* that surrounds *B* and is separated from the glass matrix (*G*) by a sharp step like boundary. This morphology complicates structural investigation by EBSD method, which works well only on very flat surfaces. So, to obtain flat surface in areas of dots the samples were repolished using Al_2O_3 suspensions. The SEM images of 5 dots induced by different laser beam exposures are shown in Fig. 3, under the conditions mentioned in the caption, as typical examples in this study. We expect that polishing the sample after exposure removed a layer of 1–2 μm thickness, and hence possibly changed the appearance of corresponding regions somewhat. Notwithstanding, inner region *B* in the *as irradiated* sample corresponds to the crater in the center of each dot after polishing. Evidently, region *A* due to higher hardness than glass matrix does not polish off as easily and therefore appears as an elliptic protrusion above the background of dots in Fig. 3.

Fig. 4(a) shows the SEM image of dot No. 1 selected for EBSD analysis. Fig. 4(b) presents an IQ color map of the selected region. Here the black and blue pixels represent non-crystallinity. Thus the area around

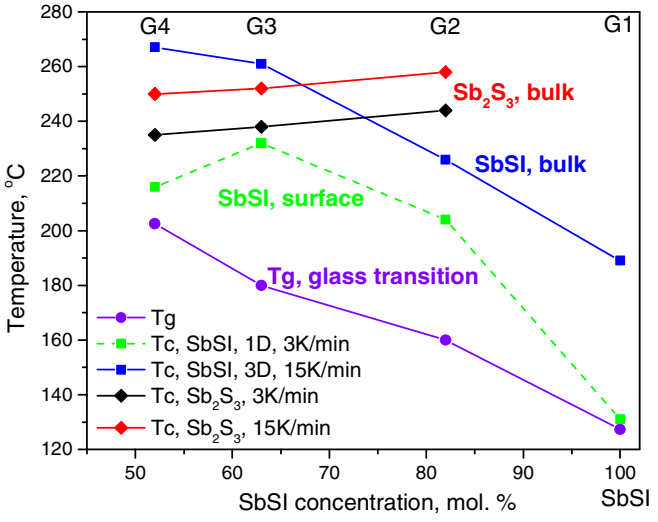

Fig. 1. Composition dependence of transformation temperatures: glass transition (circles), crystallization temperature of SbSI (squares) and Sb_2S_3 (diamonds) phases for four (G1–G4) different glasses within $xSbSI–(100–x)Sb_2S_3$ series [11,12].